Journal of Quantitative Spectroscopy & Radiative Transfer 298 (2023) 108493

Contents lists available at ScienceDirect

Journal of Quantitative Spectroscopy & Radiative Transfer

journal homepage: www.elsevier.com/locate/jqsrt

Temperature behavior of collisional parameters of oxygen fine-structure lines: O_2-O_2 case

M.A. Koshelev*, I.N. Vilkov, T.A. Galanina, E.A. Serov, D.S. Makarov, M.Yu. Tretyakov

IAP RAS, 46 Ulyanov Str., 603950 Nizhny Novgorod, Russia

ARTICLE INFO

Article history:
Received 14 November 2022
Revised 14 January 2023
Accepted 16 January 2023
Available online 18 January 2023

Keywords:
speed dependent effects
molecular oxygen
line shape
collisional parameters
temperature effect
atmospheric absorption

ABSTRACT

The microwave spectrum of oxygen, which consists of the fine-structure lines, is a tool for atmospheric research. An accurate line shape profile is necessary for modeling of the atmospheric absorption and interpreting the radiometric data. In this study, more than 500 recordings of the oxygen millimeter wave lines were obtained in a wide range of pressures (0.3–1500 Torr) and temperatures (235–357 K) using two experimental techniques that differ in principle of operation. High quality of the experimental spectra and negligible baseline allowed accurate analysis of the line shape using the quadratic speed-dependent Voigt profile. Line shape parameters for six fine-structure oxygen lines ($N = 1^+,1^-, 7^+, 11^+, 15^+$, and 19^-), including self-broadening and self-shifting, were refined. The parameters of the speed dependence of the collision relaxation rate demonstrated significantly different temperature behavior for different rotational states. In particular, the ratio γ_2/γ_0 reveals temperature independence for the lowest rotational state; the dependence becomes notable with the growth of rotational excitation. For practical use, the empirical functions were fitted to the experimental temperature and rotational dependences of the line shape parameters.

1. Introduction

Oxygen is one of the major constituents of air and responsible for a significant part of the millimeter-wave radiation absorption in the Earth's atmosphere. The O_2 spectrum in the millimeter-wave range is formed by the fine-structure lines in the ground vibrational and electronic state $X^3\Sigma_g^-$ located mostly in the range of 50–70 GHz and a single line at 118 GHz. These lines are widely used in radiometric atmospheric measurements for the temperature distribution retrieving [1] which requires absorption and radiative transfer models. The accuracy of determining the atmospheric parameters depends on the accuracy of the model and, in particular, on the underlying spectroscopic parameters of the molecular lines and the continuum [2].

In recent years, our group has made significant efforts aimed at the refinement of the line shape parameters of oxygen fine-structure lines for accurate modeling of absorption of millimeter waves by atmospheric oxygen. In particular, central frequencies [3,4], pressure broadening parameters [3,5-7] and their temperature dependences [5,8,9], and room-temperature speed-dependent parameters [7,10] were measured for lines within a wide range of rotational quantum number N using different spectroscopic techniques. Studies of collisional coupling of oxygen fine-structure lines, which were carried out with the resonator spectrometer [3,5,7,11-13], resulted in accurate line-mixing parameters.

This work continues our study of the effect of speed dependence (SD) of collisional relaxation rate and the effect of SD on the shape of the fine-structure oxygen lines. In particular, this paper is devoted to the study of the temperature variation of the SD effect for the lines which correspond to different rotational excitation of molecules. A temperature range of about 120 K centered at room temperature is considered. A wide pressure range (0.3 – 1500 Torr) is covered by two fundamentally different spectrometers having complementary abilities. The spectrometer with a radio-acoustic detector [14] was employed to register spectra of 6 lines in the range of 0.3 – 2.6 Torr. Several high-pressure spectra of the 118 GHz line were recorded from 500 to 1500 Torr using a resonator spectrometer [7,15]. Section 2 provides the details of the experiment. Section 3 demonstrates the line shape analysis of the experimental spectra. Section 4 presents the results of the study and their discussion.

2. Details of the experiment

Examples of simultaneous use of our two spectroscopic instruments for obtaining accurate and reliable parameters of molecular

* Corresponding author.
E-mail address: koma@ipfran.ru (M.A. Koshelev).

https://doi.org/10.1016/j.jqsrt.2023.108493
0022-4073/

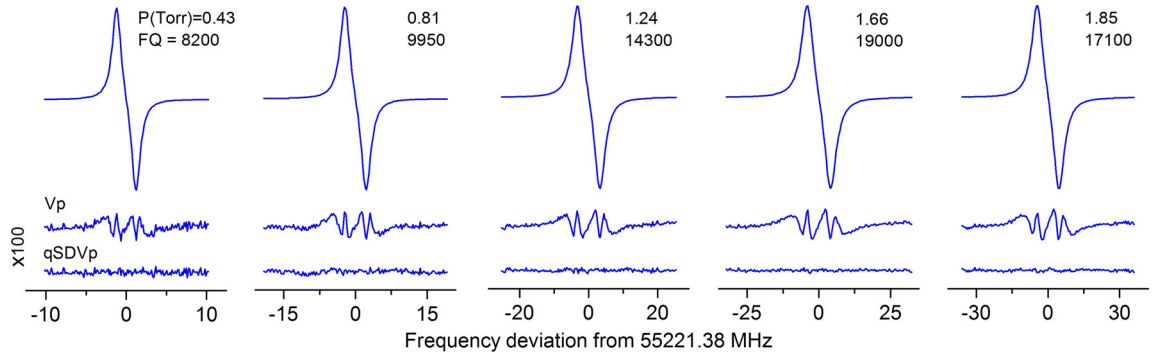

Fig. 1. Experimental recordings of the 19^- line of $^{16}O_2$ at 315 K with the RAD spectrometer. Differences (100 × zoomed) of the experimental and fitted (multifit) profiles are shown below each record for both Voigt (Vp) and SD Voigt (qSDVp) profiles. Pressure and fit quality (FQ) for qSDV profile are shown for each line recording.

spectral lines in a wide range of thermodynamic conditions can be found, e.g., in [7,10] and references therein.

The first one is a spectrometer with a frequency-stabilized backward-wave oscillator (BWO) and a radio-acoustic detector of gas absorption (RAD spectrometer). A detailed description of the spectrometer and absorption measurement method can be found in [14,16,17]. Frequency stability is determined by the GPS-tracked frequency and time standard SRS FS740. A 10 cm long single-pass copper gas cell with a sensitive microphone is isolated from external magnetic fields by a double shield made of annealed permalloy. This allows avoiding a distortion of the shape of the magnetic-dipole oxygen lines due to the Zeeman effect.

During measurements, the cell temperature was permanently controlled with *a* ±0.1 K stability around the chosen value by the Julabo FP-50 HE thermostat (http://www.julabo.de/). Four Pt100 temperature sensors (class 1/3 DIN) were mounted on the cell surface and allowed temperature measurement within ±(0.1–0.24) K depending on the reading. The gas pressure in the cell was permanently monitored using an MKS Baratron (Type 626B) gage with a range of 10 Torr which has a declared accuracy of 0.25% of the reading. The oxygen sample with a specified purity better than 99.999% was ordered from a local supplier.

The use of radiation frequency manipulation (a square-wave modulating function with a precisely known and fixed deviation) made it possible to significantly reduce the spectrometer baseline originating mainly due to the heating of the cell windows. The deviation was specified to be approximately equal to the line width. The difference in the gas absorption at frequencies defined by the BWO frequency manipulation causes pressure variations in the cell, which are registered by a capacitive microphone. The signal was further acquired by the digital lock-in amplifier with reference frequency equal to the manipulation frequency (80 Hz). The observed line shape can be modeled as

$$S(f) = F(f + dev) - F(f - dev),$$

where f is the frequency, dev is the deviation value, and $F(f)$ is the regular line shape function such as Lorentz, Voigt, etc. The line shape function was complemented by linear with frequency additive and multiplicative terms in order to account for the instrumental effects, as described in detail in [14].

A series of line profiles for each studied line were recorded at 6–9 pressures in the range of 0.3 - 2.6 Torr at a given temperature in the range from 235 to 357 K. Each line recording consisted of 201 frequency points with an acquisition time of 0.5 s per point. The final spectrum at each pressure was obtained by averaging the number (up to 40) of repeated recordings, and a signal-to-noise ratio (SNR) reached 19,500. A typical series of final spectra is shown in Fig. 1.

In order to assess the effect of standing waves in the waveguide path of the spectrometer on the measurement results and to reduce its influence, several series of spectra recordings at different pressures were obtained for a given temperature at different relative positions of the cell and the radiation source. Each series was fitted separately to determine the line shape parameters. The final value of each parameter was obtained by averaging the results of all series.

The second instrument was a resonator spectrometer [15,18] which operates at higher pressures up to 2 atm. Under such conditions, the fine-structure oxygen lines located near 60 GHz are merged in a single band, and only the 1^- fine structure line near 118 GHz can be studied as a single line.

The experimental setup and measurement method were similar to our study of this line at room temperature [7]. The spectrometer was equipped with the BWO (type OB-76) as a source of coherent continuous-wave radiation. The use of a phase-locked loop with a direct digital synthesizer allowed fast step-by-step frequency sweep without loss of the oscillation phase, providing fast recording of a resonance curve. The gas absorption coefficient was determined at the eigenmode frequencies as a term proportional to a difference in the resonance curve widths of the resonator filled with the studied gas and with a non-absorbing gas (argon).

The Fabry-Perot cavity (two spherical mirrors with a diameter of 12 cm and a radius of curvature of 49 cm, located at a distance of 51 cm from each other) is coupled with the BWO and Schottky diode-based detector by a 10 μm Polytetrafluoroethylene (PTFE) film located at an angle of 45° to the resonator axis. The resonator is placed inside the copper housing permanently connected to the Julabo FP-50 HE thermostat. The temperature of the gas sample and resonator elements is permanently monitored by eight Pt100 thermistors (1/3 DIN).

Oxygen spectra were registered at four temperatures in the range of 278–331 K. The temperature gradients of the sample along the cavity were about 0.1 K at room temperature up to 2.8 K at boundary values of the interval. Pressure in the chamber was monitored by two capacitance sensors: Pfeiffer CCR361 (1000-Torr range) and MKS Type 625B (2000-Torr range) which have stated accuracy of 0.2% and 0.25% of the reading, respectively. At a given temperature, the recording of the 1^- oxygen line was performed at five pressures in the range of 500–1500 Torr in increments of 250 Torr. Several spectra, which correspond to different distances between the waveguide system and the resonator (changing the interference pattern by analogy with the method used in [7]), were recorded for each pressure. Averaging of these spectra enabled one to decrease the impact of the parasitic reflections of radiation in the spectrometer waveguide on the experimental results. Final spectra (Fig. 2) have a typical SNR of several thousands.

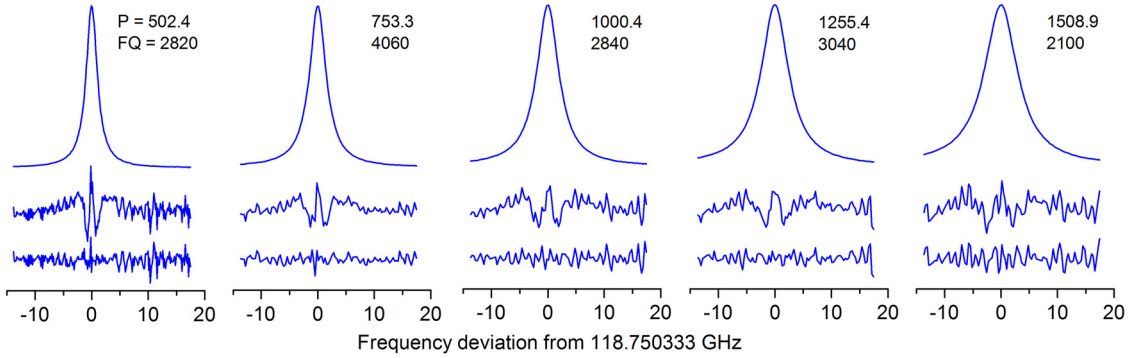

Fig. 2. Experimental recordings of the 1^- line of $^{16}O_2$ at 278 K with the resonator spectrometer. Obs.-Calc. residuals (multiplied by 100) are shown below each recording for both VVWLM and qSDVVWLM profiles. Pressure P in Torr and fit quality (FQ) in the case of qSDVVWLM profile are shown next to each line recording.

3. Line profile and spectra analysis

Spectra analysis was performed on the basis of two different line shape models with allowance for the different collisional effects manifested in the spectra registered with two spectrometers at significantly (3–4 orders of magnitude) different pressures.

For the low-pressure spectra obtained by the RAD spectrometer, the Doppler line width (HWHM), Γ_D, is at least several times less than the collisional one (Γ), but is not negligible. Therefore, the Voigt profile (Vp) was used for analysis of the RAD spectra.

At high pressures, the Doppler broadening is negligible, but the effect of line mixing becomes significant. Therefore, the spectra from the resonator spectrometer were analyzed using the Van Vleck – Weisskopf profile which was modified to account for the line-mixing effect in the first-order (in pressure) approximation (Rosenkranz profile) [19] (VVWLMp). The wing of the 60-GHz oxygen band was calculated for each experimental spectrum using the MPM code [13,20], which was modified for pure oxygen using the results of our previous measurements [3,7,9]. The calculated absorption was subtracted from the experimental spectra.

The SD effect was taken into account in the line profiles, and a quadratic dependence of line half-width Γ on the absorbing molecule speed v was assumed [21,22]:

$$\Gamma(v) = \Gamma_0 + \Gamma_2\left[\left(\frac{v}{\tilde{v}}\right)^2 - \frac{3}{2}\right], \quad (1)$$

where Γ_0 and Γ_2 are the pressure dependent parameters $\Gamma_{0,2} = \gamma_{0,2}\cdot p$, $\tilde{v} = \sqrt{2k_BT/m}$ is the most probable speed of the absorbing molecule of mass m at temperature T, and k_B is the Boltzmann's constant. The corresponding line shapes are calculated by averaging the conventional profiles using Maxwell-Boltzman distribution as a weight and are called as quadratic speed-dependent Voigt profile (qSDVp) and quadratic speed-dependent Van Vleck – Weisskopf line-mixing profile (qSDVVWLMp), respectively (Eqs. (2), (4) and (6) from [7]). The SD of pressure shifting and mixing were neglected as in our previous studies [7,9].

Data analysis was performed using the multispectrum fitting procedure, which applied the simultaneous fitting of the model function to all experimental spectra of a chosen line at a given temperature. The expected linear dependence of collisional line shape parameters (broadening, shifting, and speed dependence parameter) on pressure was constrained in the model function. This reduces the uncertainty of the results, which is related to the mutual correlation of the line shape and baseline parameters in the model function. The spectrum-by-spectrum fitting approach (which implies a separate adjustment of each line shape parameter at a given pressure and following linear approximation of derived parameters) was also applied for the data analysis. Both approaches demonstrated similar results, justifying the correctness of the model function and the negligible effect of the spectrometer baseline on the results.

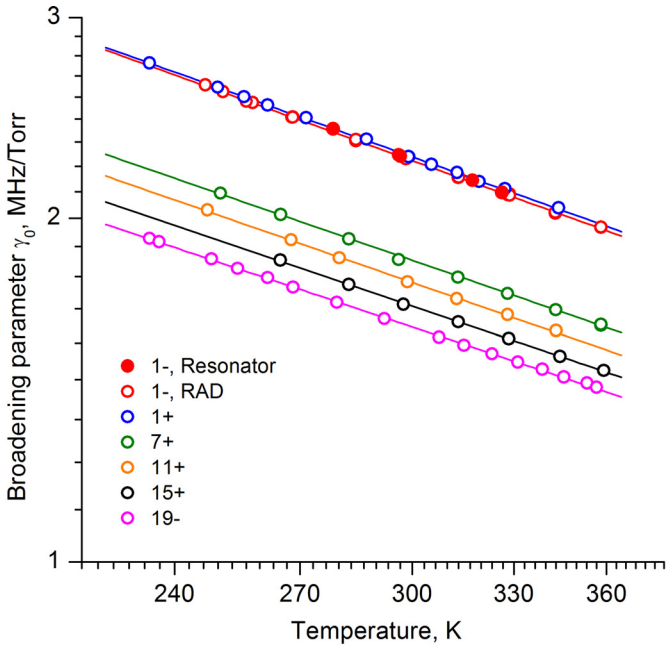

Fig. 3. Experimental temperature dependence of the self-pressure broadening parameter γ_0 for different fine-structure lines (circles). For the 1^- line, both RAD (empty circles) and resonator (filled circles) data are presented. Solid lines represent the corresponding fitted power law functions. Note log scale for both axes.

The spectra from different spectrometers were analyzed separately. Typical residuals are shown in Figs. 1 and 2, revealing characteristic w-shape discrepancy between the experimental spectra and the fitted speed-independent profiles (Vp and VVWLMp). The fitting of the SD profiles demonstrates the noise-like residuals. In total, the spectra for six fine-structure oxygen lines ($N = 1^+$,1^-, 7^+, 11^+, 15^+, and 19^-) were analyzed.

4. Results and discussions

4.1. Pressure broadening and its speed dependence

The pressure broadening and its SD parameters determined from the multifit analysis of the experimental spectra of the RAD spectrometer are presented in Figs. 3-5 as a function of temperature for all studied lines. The high-pressure data obtained for the 1^- line using the resonator spectrometer confirm the low-pressure

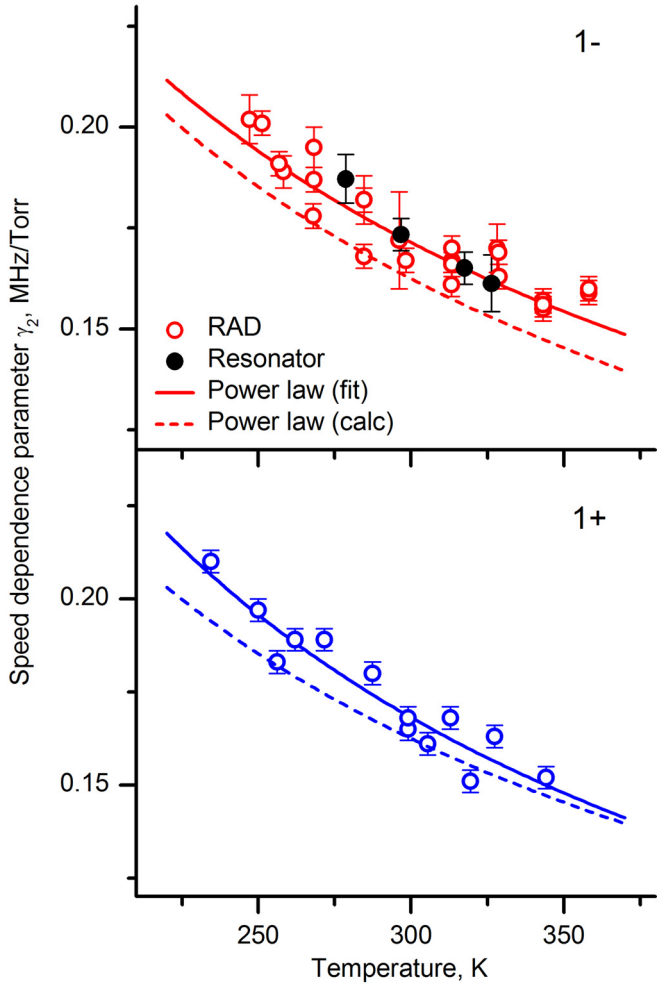

Fig. 4. Temperature behavior of the speed dependence parameter γ_2 for the 1^- and 1^+ lines. Solid lines represent the fitted power-law function. Dashed lines demonstrate the calculated T-dependences (see text for details). Error bars are $\pm 3\sigma$ fit uncertainties.

results from the RAD spectrometer. Agreement of two datasets within the experimental uncertainties shows the reliability of the experimental data. It is worth noting that the pressure broadening parameter of all the studied fine-structure lines is expectedly decreasing with the temperature increase (Fig. 3). However, the SD parameter γ_2 demonstrates significantly different qualitative temperature behavior depending on the rotational quantum number N of the transition. Thus, for the 1^- and 1^+ lines (Fig. 4) and for the 7^+ line (Fig. 5), the experimental data show a decrease in the SD parameter with an increase in temperature. For the 11^+ line, γ_2 becomes independent of temperature, and then for the lines with higher N (Fig. 5), the temperature dependence of γ_2 tends to become the opposite to the initial, i.e., on average the parameter value increases with increasing temperature. As far as we know, this behavior has been neither observed nor predicted.

Recall that all lines studied in this work correspond to transitions within different rotational levels of the O_2 molecule. The corresponding rotational energies increase rapidly with rotational excitation and become comparable to thermal energy kT for $N \approx 11$, which indicates the same state where the temperature exponent of the SD parameter changes its sign. This is probably the key to explaining the observed behavior of γ_2, however the first principle calculations are required to confirm or refute it.

An empirical power-law function was used for modeling of the temperature dependence of both pressure broadening coefficient $\gamma_0(T)$ and its speed dependence $\gamma_2(T)$:

$$X(T) = X(T_0)\left[\frac{T_0}{T}\right]^{n_x}, \quad (2)$$

where X is either γ_0 or γ_2, $T_0 = 296$ K is the reference temperature, and the temperature exponent n_x is either $n_{\gamma 0}$ or $n_{\gamma 2}$. The fitted power-law functions in Figs. 3-5 demonstrate their consistency with experimental data in the range of specified temperatures.

The pressure broadening coefficients $\gamma_0(296)$ obtained from the RAD spectrometer data are plotted in Fig. 6a as a function of the rotational quantum number N together with the results of our earlier study at room temperature [10]. Both datasets are consistent with each other, and their rotational dependence is well described by the Padé approximation determined in [10] in the wide range of N up to 39 as

$$\gamma(N) = A_\gamma + \frac{B_\gamma}{1 + \sum c_i \cdot N^i}. \quad (3)$$

We found that there is no need to adjust the coefficients of the Padé approximation for the self-broadening $\gamma(296)$ and $\gamma_0(296)$ obtained in [10], so we simply represent them in Table 1 for the completeness of the dataset.

Table 1
Coefficients of the Padé approximation (3) for the self-broadening $\gamma(296)$ and $\gamma_0(296)$ from [10] and for the $\gamma_2(296)$ determined in this study (in MHz/Torr). Note that c coefficients are the same for all three parameters.

Coefficient	$\gamma(296)$	$\gamma_0(296)$	$\gamma_2(296)$
A	0.2499	0.2519	0.0184
B	2.1588	2.1762	0.1589
c_1	$9.298 \cdot 10^{-2}$		
c_2	$-9.040 \cdot 10^{-3}$		
c_3	$4.985 \cdot 10^{-4}$		
c_4	$-1.225 \cdot 10^{-5}$		
c_5	$1.162 \cdot 10^{-7}$		

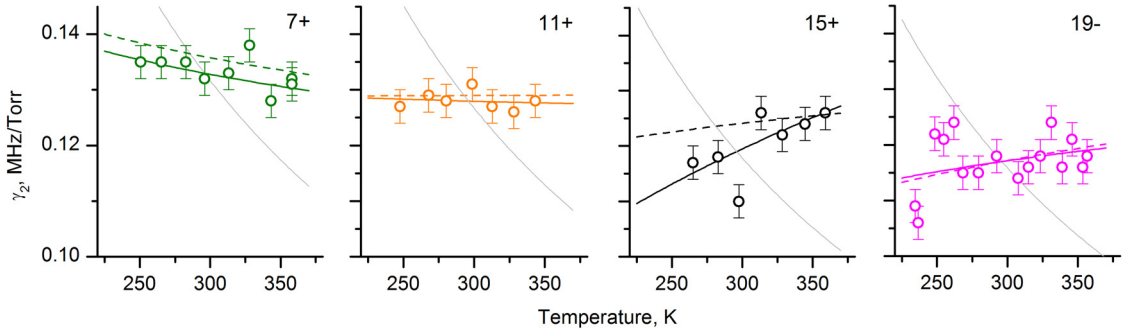

Fig. 5. The same as Fig. 4 but for 7^+, 11^+,15^+, and 19^- lines. Thin gray curves correspond to the function $\gamma_2(T) = \gamma_2(296)[\frac{296}{T}]^{n_{\gamma 0}}$.

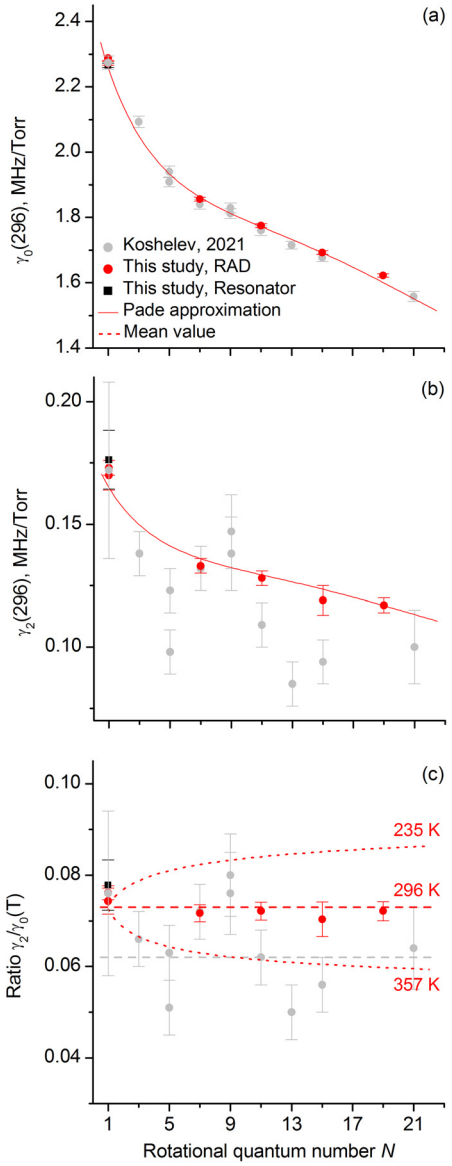

Fig. 6. Rotational behavior of the (a) pressure broadening $\gamma_0(296)$, (b) speed dependence $\gamma_2(296)$, and (c) their ratio γ_2/γ_0 at different temperatures. Red and black dots show this study data from RAD and resonator spectrometers, respectively. Gray dots correspond to our previous work [10], all datasets are at 296 K. Error bars are $\pm 3\sigma$ fit uncertainties. Solid lines are the Padé approximations (see text for details) and dashed lines are the mean values of the corresponding datasets. Dotted lines on panel (c) are the ratios calculated at 235 K and 357 K using Padé approximations and temperature dependences in Fig. 7.

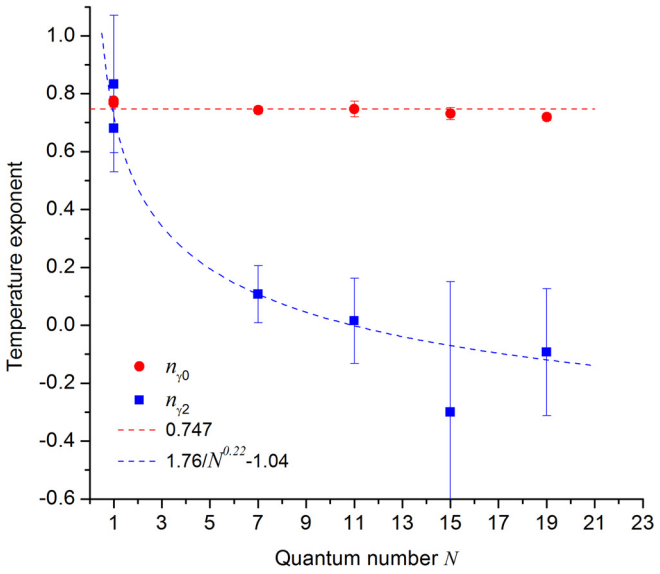

Fig. 7. Rotational behavior of the temperature exponent of pressure broadening $n_{\gamma 0}$ (red circles) and speed dependence $n_{\gamma 2}$ (blue squares). Error bars are $\pm 3\sigma$ fit uncertainties. The meaning of dashed lines is presented in the figure and described in the text.

The rotational dependence of the SD parameter $\gamma_2(296)$ was not determined in [10] due to the large spread of experimental data. The results of this study are much more accurate and confidently reveal the rotational dependence (Fig. 6b) which is qualitatively similar to that for $\gamma_0(296)$. This is confirmed by the independence of the ratio $\gamma_2(296)/\gamma_0(296)$ on the rotational quantum number N (Fig. 6c). The mean value of the ratio was determined as 0.073(2) (against 0.062(6) in [10]) and it was used for calculating the coefficients of the Padé function for $\gamma_2(296)$ shown in Table 1. The values of γ_2 measured in this study generally agree within the experimental uncertainties with our previous results [10], but some systematic difference between two datasets was observed. We believe that this difference (as well as a larger spread of experimental points) is caused by the effect of the spectrometer baseline on a line shape for the lower-quality spectra of the previous study [10].

The temperature exponents $n_{\gamma 0}$ and $n_{\gamma 2}$ obtained from the fitting of Eq. (2) to the experimental dependences $\gamma_0(T)$ and $\gamma_2(T)$, respectively, are plotted in Fig. 7 as a function of N. This demonstrates the aforementioned difference in rotational behavior of the pressure broadening and SD parameters. The exponent $n_{\gamma 0}$ is almost constant for all studied lines with a slight tendency to decrease with increasing N. The mean value of the temperature exponent was determined as $n_{\gamma 0} = 0.747(20)$ for the SD broadening and $n_{\gamma} = 0.758(15)$ for the speed-independent broadening. These values are in good agreement with $n_{\gamma} = 0.765(11)$ obtained in our earlier study [9], where the independence of the exponent from N within the measurement uncertainty was also demonstrated for both self- and air-broadening for N in the range from 1 to 19. Greater uncertainty of the temperature exponents of this study occurs from i) fewer averaged parameters (6 values in this study against 12 values in [9]) and ii) a stronger correlation of the line shape parameters in the SD profile causes a larger spread of the determined values. This N-independent behavior is adopted in the current version of the atmospheric millimeter-wave propagation model (MPM) [20], but differs from the air-broadening exponents of these lines presented in HITRAN2020 [23], where n_{γ} for the 1^- line is notably greater than for all other lines of the band (0.97 versus 0.72, respectively). Note that these data are based on experimental results obtained by Drouin [24] for the 1^- line and the 425-GHz line corresponding to the pure rotational $J_N = 3_2 \leftarrow 1_2$ transition of oxygen molecule.

Unlike $n_{\gamma 0}$, $n_{\gamma 2}$ shows a rapid decrease as N increases and changes the sign at $N = 11$. Such a variation of $n_{\gamma 2}$ means, in particular, that the ratio γ_2/γ_0 is not constant from N at different temperatures Fig. 6c) and the case of room temperature is not a general property, but simply a lucky coincidence. Note that the effect would not be possible to reveal if the uncertainty of the ratio γ_2/γ_0 was about 20% or more, which is typical at present. This is probably why, as far as we know, there have been no studies observing or predicting this behavior of the SD parameter. For practical use, the rotational dependence of the temperature exponents can be modeled using the mean value $n_{\gamma 0} = 0.747(20)$ and empirical function $n_{\gamma 2}(N) = 1.76 \,/\, N^{0.22} - 1.04$. The temperature

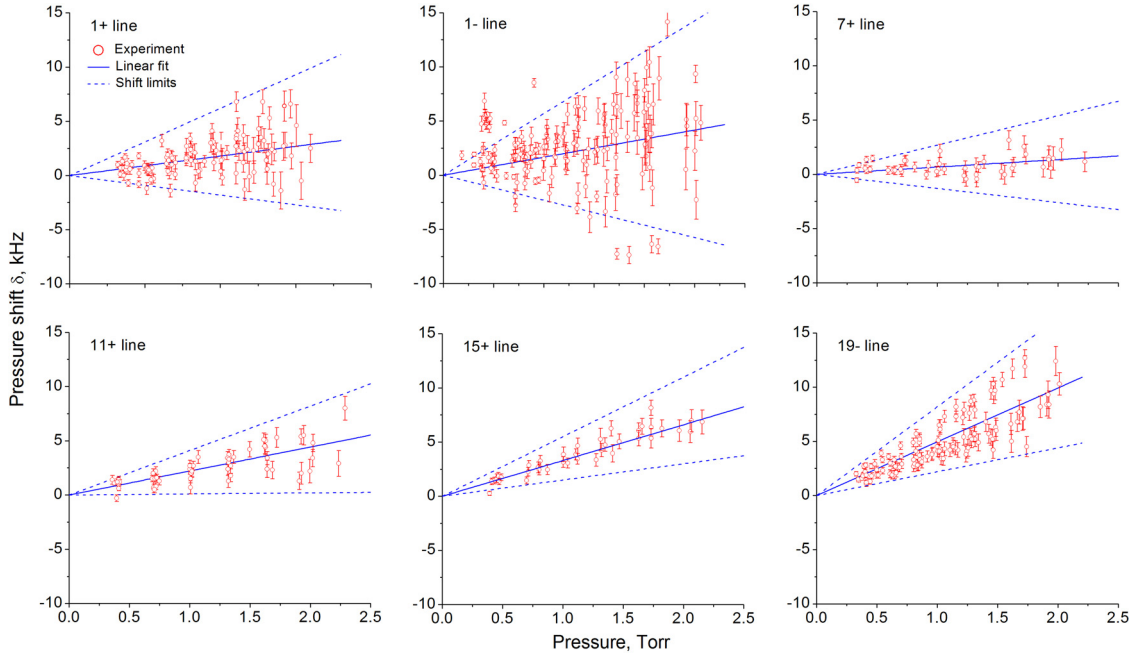

Fig. 8. Pressure behavior of the oxygen line positions obtained using RAD spectrometer. Solid lines are the results of linear regression of the experimental points. Dashed lines are the shift limits.

dependence of $\gamma_2(T)$ calculated for the studied lines using Eqs. (2) and ((3), coefficients from Table 1, and empirical rotational dependence $n_{\gamma 2}(N)$ are plotted in Figs. 4 and 5 demonstrating appropriateness of their use for practical applications. It is also shown in Fig. 5 that for lines with $N \geq 7$, the use of $n_{\gamma 0}$ instead of $n_{\gamma 2}$ leads to a significant error in determining γ_2 as we move away from room temperature.

4.2. Pressure shifting

Pressure shifts of the fine-structure oxygen lines were estimated in our previous studies [3,7,9,10] as less than ±4.5 kHz/Torr for the 1^- line and less than ±15 kHz/Torr for the other lines up to $N = 39$ [10]. However, new high-quality data allowed refining of the pressure shift coefficients and their rotational dependence.

Fig. 8 presents the manifestation of pressure shifts obtained using the RAD spectrometer and Voigt profile for the lines under study. Notable temperature behavior was not detected, therefore, the experimental points corresponding to different temperatures were plotted all together. A linear (within experimental uncertainties) growth of the line shift with increasing pressure was observed for all the lines studied, which is typical of the collision effect. Shifting parameters, which are determined as the slope of the linear pressure dependence, vary from about 1 kHz/Torr for the 1^- line up to 5 kHz/Torr for the 19^- line, which is in good agreement with our estimates given in [10]. Moreover, the revision of these earlier data made it possible to estimate the pressure shifting coefficients for the lines up to $N = 35$. Both datasets are plotted in Fig. 9 together with the resonator spectrometer value for the 1^- line. The latter point testifies to the remarkable consistency of the data obtained by different experimental techniques. In general, the data demonstrate that the shifting effect is positive ("blue shift") for all lines of the band and the shifting parameter increases up to about 15 kHz/Torr with increasing N. A similar behavior was observed for the oxygen B-band lines (see Fig. 4a in [25]), for which the collisional shift is negative ("red shift") and its absolute value increases with increasing N, although not as fast as

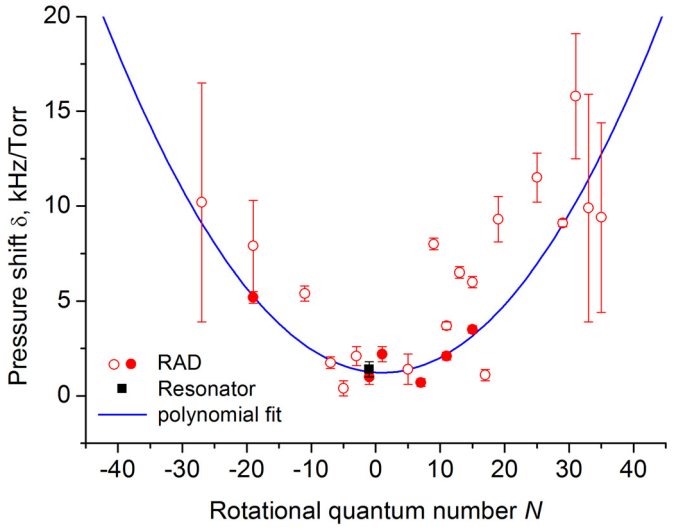

Fig. 9. Rotational dependence of the pressure self-shifting parameter for the fine-structure lines. The RAD spectrometer data are shown by circles: filled circles correspond to this study, open circles demonstrate the results of re-analysis of the data from the previous study [10]. The resonator spectrometer value for the 1^- line is shown by a black square. Error bars are $\pm 1\sigma$ fit uncertainties. Solid curve is a quadratic function fitted to the experimental data (see text for details).

for the band under study. Note that pressure shifting of the B-band lines is about 30 times greater than for the millimeter-wave lines.

The quadratic function $\delta(N) = 1.2 - 0.02N + 0.01N^2$ with numerical coefficients, which were obtained as a result of its fitting to the experimental data (Fig. 9), can be used for applications. The use of this rotational dependence of pressure shifting to determine the unshifted (zero pressure) positions of the fine-structure lines in [4] enabled us to increase by 6 times the accuracy of the molecular constants responsible for the fine structure of the rotational oxygen levels in comparison with the most recent work [26], followed by about an order of magnitude reduction of the uncertainty in predicting the frequencies of the corresponding transitions. This

Table 2
Measured parameters of the line shape of the oxygen fine-structure lines. Errors are combined total uncertainties.

Line notation $N^{\pm}$	$\gamma_0(296)$ MHz/Torr	$n_{\gamma 0}$	$\gamma_2(296)$ MHz/Torr	$n_{\gamma 2}$	δ kHz/Torr
1^-	2.272(6)	0.776(6)	0.173(3)	0.68(15)	1.0(12)
1^+	2.288(7)	0.768(15)	0.170(6)	0.83(24)	2.2(12)
7^+	1.856(6)	0.743(12)	0.133(3)	0.11(10)	0.7(6)
11^+	1.775(6)	0.747(27)	0.128(3)	0.02(15)	2.1(6)
15^+	1.692(6)	0.731(21)	0.119(6)	−0.30(45)	3.5(6)
19^-	1.622(5)	0.719(12)	0.117(3)	−0.09(22)	5.2(9)

fact also indicates that the observed shift has a collisional origin and indicates the need to take the effect for accurate modeling of the atmospheric absorption into account.

Line shape parameters of the oxygen fine-structure lines measured in this study are presented in Table 2. Combined total uncertainty of each parameter was calculated as the square root of the sum of squared errors of fitting (3σ) and pressure and temperature readings.

5. Conclusions

The study of the shape of the fine-structure oxygen lines was carried out using two spectroscopic techniques, which are different in principle of operation, in a wide pressure range of 0.3 – 1500 Torr. The temperature interval from 235 to 357 K was covered. The signal-to-noise ratio of the experimental spectra reached 19,500. Various collisional effects, which appeared in the experimental spectra at significantly different pressures, were studied including the speed dependence of collisional relaxation rate. In total, the shape of six oxygen lines with N varying from 1 to 19 was analyzed. The results of this study confirmed the rotational dependence of the pressure broadening $\gamma_0(296)$ previously determined in our study [10] at room temperature. For the speed-dependence parameter $\gamma_2(296)$, the rotational dependence was refined.

The temperature behavior of $\gamma_2(T)$ was studied for the first time. It was demonstrated that the power law is suitable for both $\gamma_0(T)$ and $\gamma_2(T)$ in the studied temperature range. However, the corresponding temperature exponents $n_{\gamma 0}$ and $n_{\gamma 2}$ showed significantly different rotational dependence. Namely, $n_{\gamma 0}$ is almost independent of N, while $n_{\gamma 2}$ decreases rapidly with increasing N, changing the sign to the opposite at $N = 11$. Empirical functions were suggested for modeling of the temperature and rotational dependences of the line shape parameters of the fine-structure lines.

The first measurement of the rotational dependence of the collisional shifting of oxygen lines led to a multiple improvement in the accuracy of the line positions and molecular fine-structure constants [4] confirming collisional origin of the observed effect. Obtained rotational dependence is in good qualitative agreement with the B-band data known from the literature.

The results of the study can be used for refining radiation propagation models and may serve for testing fast developing methods of *ab initio* calculations of collisional line shape parameters [27].

Declaration of competing interest

The authors declare that they have no known competing financial interests or personal relationships that could have appeared to influence the work reported in this paper.

CRediT authorship contribution statement

M.A. Koshelev: Methodology, Investigation, Formal analysis, Writing – original draft, Writing – review & editing. **I.N. Vilkov:** Investigation, Data curation. **T.A. Galanina:** Investigation, Data curation. **E.A. Serov:** Investigation, Data curation. **D.S. Makarov:** Visualization, Software. **M.Yu. Tretyakov:** Supervision, Conceptualization, Writing – original draft, Writing – review & editing.

Data Availability

Data will be made available on request.

Acknowledgments

The authors thank P.W. Rosenkranz for discussing the results. Research was carried out using the Large-scale research facilities «СКР-7» (USU №3589084). The study was supported by the Russian State project No 0030–2021–0016. The study with the resonator spectrometer was supported by the Russian Science Foundation (project No. 18–72–10113, https://rscf.ru/en/project/18–72–10113/).

References

[1] Wulfmeyer V, Hardesty RM, Turner DD, Behrendt A, Cadeddu MP, Di Girolamo P, Schlüssel P, Van Baelen J, Zus F. A review of the remote sensing of lower tropospheric thermodynamic profiles and its indispensable role for the understanding and the simulation of water and energy cycles. Rev Geophys 2015;53:819–95. doi:10.1002/2014RG000476.
[2] Cimini D, Rosenkranz PW, Tretyakov MYu, Koshelev MA, Romano F. Uncertainty of atmospheric microwave absorption model: impact on ground-based radiometer simulations and retrievals. Atmos Chem Phys 2018;18:15231–59. doi:10.5194/acp-18-15231-2018.
[3] Tretyakov MYu, Koshelev MA, Dorovskikh VV, Makarov DS, Rosenkranz PW. 60-GHz oxygen band: precise broadening and central frequencies of fine structure lines, absolute absorption profile at atmospheric pressure, revision of mixing coefficients. J Molec Spectrosc 2005;231:1–14.
[4] Koshelev MA, Golubiatnikov GYu, Vilkov IN, Tretyakov MYu. Molecular oxygen fine structure with sub-kHz accuracy. J Quant Spectrosc Radiative Transfer 2022;278:108001.
[5] Makarov DS, Koval IA, Koshelev MA, Parshin VV, Tretyakov MYu. Collisional parameters of the 118-GHz oxygen line: temperature dependence. J Molec Spectrosc 2008;252:242–3.
[6] Koshelev MA, Vilkov IN, Tretyakov MYu. Pressure broadening of oxygen fine structure lines by water. J Quant Spectrosc Radiat Transf 2015;154:24–7.
[7] Koshelev MA, Delahaye T, Serov EA, Vilkov IN, Boulet C, Tretyakov MYu. Accurate modeling of the diagnostic 118-GHz oxygen line for remote sensing of the atmosphere. J Quant Spectrosc Radiat Transf 2017;196:78–86.
[8] Tretyakov MYu, Koshelev MA, Koval I, Parshin VV, Kukin LM, Fedoseev LI, et al. Temperature dependence of pressure broadening of the N=1− fine structure oxygen line at 118.75GHz. J Molec Spectrosc 2007;241(1):109–11.
[9] Koshelev MA, Vilkov IN, Tretyakov MYu. Collisional broadening of oxygen fine structure lines: the impact of temperature. J Quant Spectrosc Radiat Transf 2016;169:91–5.
[10] Koshelev MA, Vilkov IN, Makarov DS, Tretyakov MYu, Rosenkranz PW. Speed-dependent broadening of the O_2 fine-structure lines. J. Quant. Spectrosc. Radiative Transfer 2021;264:107546.
[11] Tretyakov MYu, Golubiatnikov GYu, Parshin VV, Koshelev MA, Myasnikova SE, Krupnov AF, et al. Experimental study of the line mixing coefficient for 118.75GHz oxygen line. J Molec Spectrosc 2004;223:31–8.
[12] Makarov DS, Tretyakov MYu, Rosenkranz PW. 60-GHz oxygen band: precise experimental profiles and extended absorption modeling in a wide temperature range. J Quant Spectrosc Radiat Transf 2011;112(9):1420–8.
[13] Makarov DS, Tretyakov MYu, Rosenkranz PW. Revision of the 60-GHz atmospheric oxygen absorption band models for practical use. J Quant Spectrosc Radiat Transf 2020;243:106798.
[14] Tretyakov MYu, Koshelev MA, Makarov DS, Tonkov MV. Precise measurements of collision parameters of spectral lines with a spectrometer with radioacoustic detection of absorption in the millimeter and submillimeter ranges. Instrum Exp Tech 2008;51:78–88.
[15] Tretyakov MYu, Krupnov AF, Koshelev MA, Makarov DS, Serov EA, Parshin VV. Resonator spectrometer for precise broadband investigations of atmospheric absorption in discrete lines and water vapor related continuum in millimeter wave range. Rev Sci Instr 2009;80:093106.

[16] Krupnov A.F., Burenin A.V. New methods in submillimeter microwave spectroscopy. in "Molecular spectroscopy: modern research" v.2, K.N. Rao, Ed., pp. 93–126, Academic Press, N.Y.(1976).
[17] Krupnov A.F. Modern submillimetre microwave scanning spectrometry. In "Modern aspects of microwave spectroscopy", G.W. Chantry, editor, pp. 217–56, Academic Press, L. (1979).
[18] Koshelev MA, Leonov II, Serov EA, Chernova AI, Balashov AA, Bubnov GM, Andriyanov AF, Shkaev AP, Parshin VV, Krupnov AF, Tretyakov MYu. New frontiers of modern resonator spectroscopy. IEEE Trans. on THz Sci. Technol. 2018;8(6):773–83.
[19] Rosenkranz PW. Shape of the 5mm oxygen band in the atmosphere. IEEE Trans Antennas Propag 1975;23(4):498–506.
[20] Rosenkranz P.W. Line-by-line microwave radiative transfer (non-scattering), DOI: 10.21982/M81013 https://tools.grss-ieee.org/rscl1/coderecord.php?id=483
[21] Rohart F, Mader H, Nicolaisen HW. Speed dependence of rotational relaxation induced by foreign gas collisions: studies on CH_3F by millimeter wave coherent transients. J Chem Phys 1994;101(8):6475–86.
[22] Rohart F, Ellendt A, Kaghat F, Mäder H. Self and polar foreign gas line broadening and frequency shifting of CH_3F: effect of the speed dependence observed by millimeter-wave coherent transients. J Molec Spectrosc 1997;185(2):222–33.
[23] Gordon IE, Rothman LS, Hargreaves RJ, Hashemi R, Karlovets EV, Skinner FM, et al. The HITRAN2020 molecular spectroscopic database. J Quant Spectrosc Radiat Transf 2022;277:107949. doi:10.1016/j.jqsrt.2021.107949.
[24] Drouin BJ. Temperature dependent pressure induced linewidths of $^{16}O_2$ and $^{18}O^{16}O$ transitions in nitrogen, oxygen and air. JQSRT 2007;105:450–8.
[25] Domysławska J, Wójtewicz S, Masłowski P, Cygan A, Bielska K, Trawiński RS, Ciuryło R, Lisak D. A new approach to spectral line shapes of the weak oxygen transitions for atmospheric applications. J Quant Spectrosc Radiat Transf 2016;169:111–21.
[26] Drouin BJ, Yu S, Miller CE, Müller HSP, Lewen F, Brünken S, et al. Terahertz spectroscopy of oxygen, O_2, in its $^3Sigma^-_g$ and ^1Delta electronic states: THz Spectroscopy of O_2. J Quant Spectrosc Radiat Transf 2010;111:1167–73.
[27] Gancewski M, Jóźwiak H, Quintas-Sánchez E, Dawes R, Thibault F, Wcisło P. Fully quantum calculations of O_2–N_2 scattering using a new potential energy surface: collisional perturbations of the oxygen 118GHz fine structure line. J Chem Phys 2021;155:124307. doi:10.1063/5.0063006.